Yield-Driven Electromagnetic Optimization via Multilevel Multidimensional Models

John W. Bandler, *Fellow, IEEE,* Radoslaw M. Biernacki, *Senior Member, IEEE,* Shao Hua Chen, *Member, IEEE,* Piotr A. Grobelny, and Shen Ye, *Member, IEEE*

Abstract—**We present the foundation of a sophisticated hierarchical multidimensional response surface modeling system for efficient yield-driven design. Our scheme dynamically integrates models and database updating in real optimization time. The method facilitates a seamless, smart optimization-ready interface. It has been specially designed to handle circuits containing complex subcircuits or components whose simulation requires significant computational effort. This approach makes it possible, for the first time, to perform direct gradient-based yield optimization of circuits with components or subcircuits simulated by an electromagnetic simulator. The efficiency and accuracy of our technique are demonstrated by yield optimization of a three-stage microstrip transformer and a small-signal microwave amplifier. We also perform yield sensitivity analysis for the three-stage microstrip transformer.**

I. Introduction

A NEW multilevel multidimensional response surface modeling technique is presented for effective and efficient yield-driven design. This approach makes it possible, for the first time, to perform yield optimization as well as yield sensitivity analysis of circuits with microstrip structures simulated by an electromagnetic (EM) simulator.

Yield-driven design is now recognized as effective, not only for massively manufactured circuits but also to ensure first-pass success in any design where the prototype development is lengthy and expensive. The complexity of calculations involved in yield optimization requires special numerical techniques, e.g., [1]–[4]. In this paper we extend our previously published [2], [4], highly efficient quadratic interpolation technique to dynamic multilevel response surface modeling. It has been specially designed to handle circuits containing complex subcircuits or components whose simulation requires significant computational effort.

With the increasing availability of EM simulators [5]–[7] it is very tempting to include them into performance-driven and even yield-driven circuit optimization. However, direct utilization of EM simulation for yield optimization or sensitivity analysis might seem to be computationally prohibitive. By constructing what we call local Q-models for each component simulated by an EM simulator we effectively overcome the computational burden of repeated EM simulations, which would otherwise be invoked for many statistical circuit outcomes throughout all yield optimization iterations. To maintain high accuracy, the Q-models are automatically updated whenever an outcome leaves the validity region of the current Q-model.

We show that when the proposed multilevel Q-modeling technique is used together with expensive, but more accurate simulations at the component level, the results are more reliable than those obtained from traditional analytical/empirical component simulations.

Efficiency and accuracy of our technique are demonstrated by yield optimization of a three-stage microstrip transformer and a small-signal amplifier. For the three-stage microstrip transformer we additionally perform yield sensitivity analyses and investigate different sets of optimization variables. Optimization was performed within the OSA90/hope™ [8] simulation-optimization environment with Empipe™ [9] driving ***em***™ [7] on a Sun SPARCstation 1+. We used the OSA90/hope one-sided ℓ_1 optimizer [10] for yield optimization.

II. Efficient Q-Modeling

A. Formulation of the Method

The Q-model of a generic response $f(\boldsymbol{x})$, i.e., any response or gradient function for which we want to build and utilize the model, is a multidimensional quadratic polynomial of the form

$$q(\boldsymbol{x}) = a_0 + \sum_{i=1}^{n} a_i(x_i - r_i) + \sum_{\substack{i=1 \\ j \geq i}}^{n} a_{ij}(x_i - r_i)(x_j - r_j) \tag{1}$$

Manuscript received March 29, 1993; revised June 16, 1993. This work was supported in part by Optimization Systems Associates Inc., and in part by the Natural Sciences and Engineering Research Council of Canada under Grants OGP0007239, OGP0042444, and STR0117819. Additional support was provided through a Natural Sciences and Engineering Research Council of Canada Industrial Research Fellowship granted to S. Ye.

J. W. Bandler, R. M. Biernacki, and S. H. Chen are with the Simulation Optimization Systems Research Laboratory, Department of Electrical and Computer Engineering, McMaster University, Hamilton, Ont., Canada L8S 4L7 and Optimization Systems Associates Inc., P.O. Box 8083, Dundas, Ont., Canada L9H 5E7.

P. A. Grobelny is with the Simulation Optimization Systems Research Laboratory, Department of Electrical and Computer Engineering, McMaster University, Hamilton, Ont., Canada L8S 4L7.

S. Ye was with Optimization Systems Associates Inc., P.O. Box 8083, Dundas, Ont., Canada L9H 5E7. He is now with Com Dev Ltd., Cambridge, Ont., Canada N1R 7H6.

IEEE Log Number 9212999.

0018-9480/93$03.00

where $x = [x_1 \ x_2 \ \cdots \ x_n]^T$ is the vector of generic parameters in terms of which the response is defined, and $r = [r_1 \ r_2 \ \cdots \ r_n]^T$ is a chosen reference point in the parameter space.

To build the Q-model we use $n + 1 \le m \le 2n + 1$ base points at which the function $f(x)$ is evaluated. The reference point r is selected as the first base point x^1. The remaining $m - 1$ base points are selected by perturbing one variable at a time around r, namely,

$$x^{i+1} = r + [0 \ \cdots \ 0 \ \beta_i \ 0 \ \cdots \ 0]^T, \quad i = 1, 2, \cdots, n \tag{2}$$

$$x^{n+1+i} = r + [0 \ \cdots \ 0 \ -\beta_i \ 0 \ \cdots \ 0]^T, \quad i = 1, 2, \cdots, m - (n+1) \tag{3}$$

where β_i is a predetermined perturbation. If a variable is perturbed twice the second perturbation is located symmetrically w.r.t. r. We have applied the maximally flat quadratic interpolation (MFQI) technique [2] to such a set of base points (see [3], [4] for details). MFQI builds the Q-model by minimizing in the least-squares sense all the second-order term coefficients in (1). It is intuitively equivalent to constructing an interpolation that has the smallest deviation from the linear interpolation.

B. Implementation

Applying MFQI to the base points defined by r, (2), and (3) and reordering the variables such that the first $m - (n + 1)$ variables are perturbed twice yields the following formulas for the coefficients in (1):

$$a_{ii} = \frac{1}{2\beta_i^2}[f(x^{n+1+i}) + f(x^{i+1}) - 2f(r)], \quad i = 1, 2, \cdots, m - (n+1) \tag{4a}$$

$$a_{ii} = 0, \quad i = m - n, \cdots, n, \ m \ne 2n + 1 \tag{4b}$$

and

$$a_{ij} = 0, \quad i, j = 1, 2, \cdots, n, \ i \ne j. \tag{4c}$$

The coefficients a_0 and a_i are given by

$$a_0 = f(r) \tag{5}$$

$$a_i = \frac{1}{2\beta_i}[-f(x^{n+1+i}) + f(x^{i+1})], \quad i = 1, 2, \cdots, m - (n+1) \tag{6a}$$

and

$$a_i = \frac{1}{\beta_i}[f(x^{i+1}) - f(r)], \quad i = m - n, \cdots, n, \ m \ne 2n + 1. \tag{6b}$$

Substituting (4), (5) and (6) into (1) results in the following formula for the Q-model $q(x)$

$$q(x) = f(r) + \sum_{i=1}^{m-(n+1)} \{[f(x^{i+1}) - f(x^{n+1+i}) + (f(x^{i+1}) + f(x^{n+1+i}) - 2f(r))(x_i - r_i)/\beta_i](x_i - r_i)/(2\beta_i)\} + \sum_{i=m-n}^{n} \{[f(x^{i+1}) - f(r)](x_i - r_i)/\beta_i\}. \tag{7}$$

It is important to realize that the variable number of base points m offers a trade-off between the accuracy and cost of circuit analysis. Reducing the number of base points decreases the number of function evaluations. However, perturbing a variable only once results in a linear rather than quadratic interpolation w.r.t. that variable. This provides a spectrum of available models from a linear model (L-model), for $m = n + 1$, to a quadratic model w.r.t. all variables for $m = 2n + 1$.

The simplicity of (7) results in high efficiency of the approach. It should be noted that the computational effort increases only linearly with the number of variables n.

To apply a gradient-based optimizer we need to provide the gradients of functions $q(x)$ that are actually used by the optimizer. Differentiating (7) w.r.t. x_i results in

$$\partial q(x)/\partial x_i = [(f(x^{i+1}) - f(x^{n+1+i}))/2 + (f(x^{i+1}) + f(x^{n+1+i}) - 2f(r))(x_i - r_i)/\beta_i]/\beta_i \quad i = 1, \cdots, m - (n+1) \tag{8a}$$

and

$$\partial q(x)/\partial x_i = [f(x^{i+1}) - f(r)]/\beta_i, \quad i = m - n, \cdots, n, \ m \ne 2n + 1 \tag{8b}$$

which again is very efficient.

C. Linear Versus Quadratic Modeling

We use a simple example in which we approximate the response of a microstrip line simulated as a two-port network by the ***em*** [7] simulator.

We fix the width of the microstrip line and sweep its length l with a step Δl. First, we simulate the circuit at each point in the sweep. This provides us with the response reference data. Subsequently, we use both L- and Q-models to approximate responses at *every other* sweep point using adjacent sweep points as the model base points. Fig. 1 summarizes the results. It shows the real part of S_{11} with l swept from 3.2 to 3.8 mm and $\Delta l = 0.1$ mm. The responses for $l = 3.3$, 3.5, and 3.7 mm are modeled. The L-model uses responses at two adjacent points to model the response at the point in between, e.g., responses at points 3.2 and 3.4 mm are used to model the

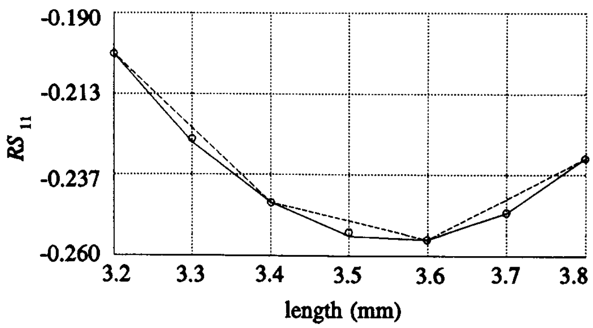

Fig. 1. Comparison between linear (dashed line) and quadratic (solid line) approximations of the real part of S_{11} of a microstrip line simulated by the *em* [7] simulator (circles).

response at 3.3 mm. The Q-model uses three points, e.g., responses at points 3.4, 3.6, and 3.8 mm are used to model the response at 3.7 mm. It can be seen that the Q-model is more accurate than the L-model.

III. Multilevel Simulation and Modeling

A. Multilevel Modeling

Multilevel modeling is depicted schematically in Fig. 2. The circuit under consideration is divided into subcircuits, possibly in a hierarchical manner. At the lowest level we have circuit components, e.g., a lumped capacitor or a microstrip structure.

Defining f_c, f_s and f_e as circuit, subcircuit and component responses, respectively, we can express the response of the circuit as a function of the subcircuit responses that are in turn functions of component responses. This hierarchy can be expressed formally as

$$f_c = f_c(f_{s1}, f_{s2}, \cdots, f_{sn_s}) \tag{9}$$

$$f_{si} = f_{si}(f_{ei1}, f_{ei2}, \cdots, f_{ein_{ei}}), \qquad i = 1, 2, \cdots, n_s \tag{10}$$

and

$$f_{eij} = f_{eij}(\boldsymbol{x}), \qquad i = 1, 2, \cdots, n_s, \qquad j = 1, 2, \cdots, n_{ei} \tag{11}$$

where n_s is the number of subcircuits and n_{ei} is the number of components in the ith subcircuit. $\boldsymbol{x}$ is the vector of circuit parameters. The responses are typically frequency-domain functions of multiport responses.

We can create a single Q-model for the overall circuit. We can also create a hierarchy of Q-models to represent some or all of the subcircuits and components, as illustrated in Fig. 2.

If the base points of a Q-model are given as $\boldsymbol{x}^1$, $\boldsymbol{x}^2$, $\cdots$, $\boldsymbol{x}^m$, where $\boldsymbol{x}^1$ is treated as the reference point $\boldsymbol{r}$ [see (2) and (3)] and $n + 1 \le m \le 2n + 1$, with n being the number of model parameters, then we can express the simulation results at these base points as

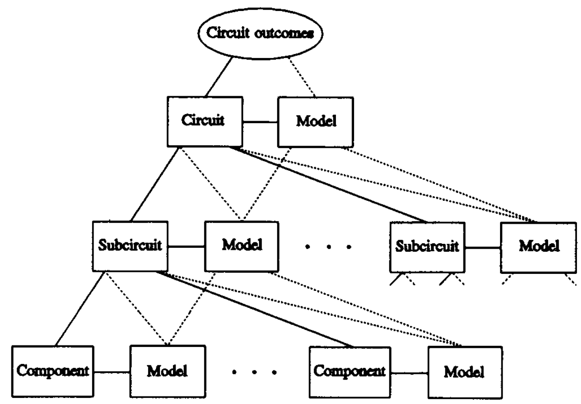

Fig. 2. Schematic diagram illustrating multilevel modeling for yield-driven optimization. Solid and dotted lines distinguish between simulated and modeled responses, respectively.

$$[\boldsymbol{f}(\boldsymbol{x}^1) \;\; \boldsymbol{f}(\boldsymbol{x}^2) \;\; \cdots \;\; \boldsymbol{f}(\boldsymbol{x}^m)] \tag{12}$$

with

$$\boldsymbol{f}(\boldsymbol{x}^i) = [f_1(\boldsymbol{x}^i) \;\; f_2(\boldsymbol{x}^i) \;\; \cdots \;\; f_k(\boldsymbol{x}^i)]^T, \qquad i = 1, 2, \cdots, m \tag{13}$$

where k is the total number of different responses. $\boldsymbol{f}$ can include a response of either circuit, subcircuit, or a component. Then

$$\boldsymbol{f}(\boldsymbol{x}) \approx \boldsymbol{q}(\boldsymbol{x}) = [q_1(\boldsymbol{x}) \;\; q_2(\boldsymbol{x}) \;\; \cdots \;\; q_k(\boldsymbol{x})]^T. \tag{14}$$

The Q-models in (14) approximate $\boldsymbol{f}(\boldsymbol{x})$ for $\boldsymbol{x}$ belonging to the Q-model validity region centered around the reference point $\boldsymbol{r} = \boldsymbol{x}^1$.

B. Implementation

During optimization the design center moves, and so does the set of associated statistical outcomes. This may result in moving some or even all of the statistical outcomes out of the validity region of the current Q-models. In the present implementation the validity region $\boldsymbol{V}$ is defined as

$$\boldsymbol{V} = \{\boldsymbol{x} \mid -\beta_i/2 < (x_i - r_i) \le \beta_i/2, \qquad i = 1, 2, \cdots, n\} \tag{15}$$

where β_i is the perturbation used in (2) and (3) to compute the model base points. To use the model for a point outside the current $\boldsymbol{V}$ requires that the Q-models in (14), and hence $\boldsymbol{V}$, be appropriately updated. We have developed an updating scheme in which the Q-models are updated automatically in real optimization time. If a statistical outcome is outside the current V, a new set of base points is generated and the responses at these base points are simulated *but only if they have not been simulated previously*. Updated Q-models follow immediately from recomputing (7). Our Q-model updating scheme is based on a database system storing results for newly simulated base points and providing extremely fast access to the results for already simulated base points. The database and Q-models are updated whenever new results become available.

If all components, subcircuits, and the overall circuit were to be simulated rather than modeled the evaluation of the circuit response f_c could proceed as follows.

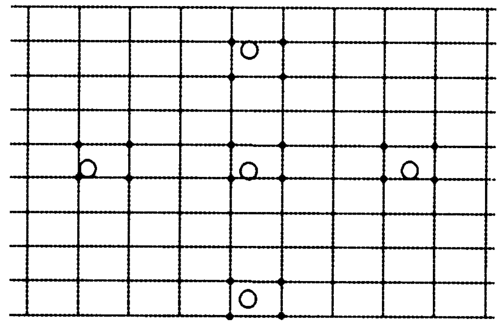

Fig. 3. Illustration of base points and discrete points. The large circles represent possible locations of base points w.r.t. a grid. The solid dots indicate discrete simulation points on the grid. If the base points are snapped to the grid, the number of simulations can be significantly reduced.

```
for the ith subcircuit, i = 1, 2, · · · , n_s {
        for the jth component in the ith subcircuit, j = 1, 2, · · · , n_ei {
                find f_eij by simulating the component according to (11);
        }
        find f_si according to (10);
}
find f_c according to (9);
```

Applying this algorithm to yield estimation or optimization may become prohibitive, especially if an EM simulator is to be used. Replacing costly circuit simulations with model evaluations yields an alternative algorithm.

```
if circuit model q_c exists
        evaluate q_c;
else {
        for the ith subcircuit, i = 1, 2, · · · , n_s {
                if subcircuit model q_si exists {
                        evaluate q_si;
                }
                else {
                        for the jth component in the ith subcircuit, j = 1, 2, · · · , n_ei {
                                if component model q_eij exists {
                                        evaluate q_eij;
                                }
                                else {
                                        find f_eij by simulating the component according to (11);
                                }
                        }
                        find f_si according to (10);
                }
        }
        find f_c according to (9);
}
```

Here, some of the responses f_{eij}, f_{si} or f_c are replaced by the corresponding models q_{eij}, q_{si}, or q_c.

C. Discrete Parameters

The circuit, subcircuits, and components may contain discrete parameters. For discrete parameters simulation can only be performed at discrete values located on the grid, as illustrated in Fig. 3. Normally, the reference vector r is taken as the nominal point x^1. This is likely to be off-the-grid. Similarly, the other base points x^{i+1} and x^{n+1+i} are likely to be off-the-grid. Local interpolation involving several simulations on the grid in the vicinity of each of the base points must then be performed. In order to avoid these excessive simulations those base points are modified to snap to the grid.

IV. Yield Optimization of a Three-Section Microstrip Transformer

A. The Transformer

A three-section 3 : 1 microstrip impedance transformer is shown in Fig. 4. The source and load impedances are 50 and 150 ohms, respectively. The design specification is set for input reflection coefficient as

$$|S_{11}| \leq 0.12 \text{ from 5 to 15 GHz.}$$

The error functions for yield optimization are calculated for frequencies from 5 to 15 GHz with a 0.5 GHz step. The transformer is built on a 0.635 mm thick substrate with relative dielectric constant 9.7.

For EM simulators, the circuit is typically partitioned into components that are defined to encompass parts of the structure that can be isolated from the other parts. This can significantly increase the efficiency of EM simulation.

The transformer was decomposed into three components, each corresponding to a different section of the transformer. In order to account for the discontinuity effects the first two sections were simulated as step discontinuities and the last section as a microstrip line. Each of the components is simulated as a two-port network.

As a verification, we also simulated the entire transformer structure as one piece. The results of simulating the circuit at the nominal minimax solution using the two methods are virtually the same.

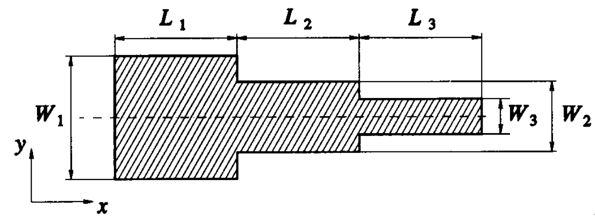

Fig. 4. The three-section 3 : 1 microstrip impedance transformer. The thickness and dielectric constant of the substrate are 0.635 mm and 9.7, respectively.

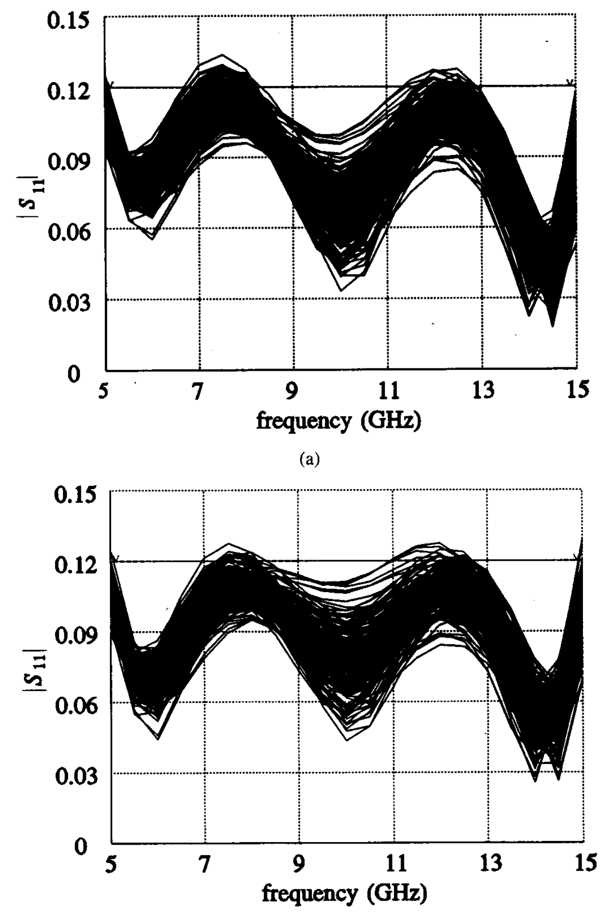

Fig. 5. Modulus of the reflection coefficient of the three-section microstrip impedance transformer versus frequency: (a) before and (b) after yield optimization. Yield is increased from 71 to 86 percent after optimization using single-level (component) Q-models.

B. Yield Optimization with Six Optimization Variables

We start yield optimization from the solution of a nominal design with W_1, W_2, W_3, L_1, L_2, and L_3 as variables. Normal distributions with 2 percent standard deviations were assumed for W_1, W_2, and W_3 and 1 percent standard deviations for L_1, L_2, and L_3. Three component-level Q-models were established for each section of the transformer at the nominal point using ***em*** [7]. The Q-models were updated during the optimization process whenever necessary.

Utilizing these Q-models we conducted two experiments to demonstrate multilevel Q-modeling: 1) yield optimization using single-level (component) modeling and 2) yield optimization using two-level (component and circuit response) modeling. 100 statistical outcomes were used for yield optimization. The solutions in both cases are almost identical: yield (estimated by 250 outcomes) is increased from 71 to 86 percent using single-level modeling and to 85 percent using two-level modeling. Fig. 5(a) illustrates the Monte Carlo sweep before optimization and Fig. 5(b) shows the corresponding sweep after yield optimization using single-level (component) modeling. The values of the optimization variables before and after yield optimization for both single- and two-level modeling are given in Table I. The solution of design centering is quite close to the nominal minimax design. This is expected, taking into account the small tolerances on the parameters.

CPU time for yield optimization, performed on a Sun SPARCstation 1+, was 16 min for single-level modeling and 3 min when two-level Q-models were used. Elapsed time for the ***em*** [7] simulations using single-level modeling was about 100 h. The two-level modeling approach exploited the database created during single-level optimization and did not require any additional ***em*** [7] simulations.

TABLE I
MICROSTRIP PARAMETERS OF THE THREE-SECTION MICROSTRIP TRANSFORMER (SIX VARIABLES)

Parameters[a]	Nominal design	Centered design[b]	Centered design[c]
W_1	0.4294	0.4363	0.4377
W_2	0.2080	0.2055	0.2053
W_3	0.07	0.07	0.07
L_1	3.0	2.951	2.8875
L_2	3.0	2.998	3.0007
L_3	3.0	3.046	3.058
Yield[d]	71 percent	86 percent	85 percent

[a]Parameters are in millimeters.
[b]Single-level modeling.
[c]Two-level modeling.
[d]100 outcomes were used in yield optimization and 250 outcomes for yield verification.

TABLE II
MICROSTRIP PARAMETERS OF THE THREE-SECTION MICROSTRIP TRANSFORMER (THREE VARIABLES)

Parameters[a]	Nominal design	Centered design[b]	Centered design[c]
W_1	0.4294	0.4339	0.4333
W_2	0.2080	0.2081	0.2079
W_3	0.07	0.07	0.07
L_1	3.0[d]	3.0[d]	3.0[d]
L_2	3.0[d]	3.0[d]	3.0[d]
L_3	3.0[d]	3.0[d]	3.0[d]
Yield[e]	71 percent	79 percent	78 percent

[a]Parameters are in millimeters.
[b]Single-level modeling.
[c]Two-level modeling.
[d]Not optimized.
[e]100 outcomes were used in yield optimization and 250 outcomes for yield verification.

C. Yield Optimization with Three Optimization Variables

We investigated yield optimization with W_1, W_2, and W_3 as variables. L_1, L_2, and L_3 were not optimized. The solutions obtained using component and both component and circuit modeling are again very similar. Yield is increased to 79 percent with component-level Q-models and to 78 percent with component- and circuit-level Q-models. Parameter values for both solutions are listed in Table II. The CPU time was 5 min for component-level and 41 s for two-level Q-modeling. The previously established database was sufficient for this experiment, so that no additional ***em*** [7] simulations were required.

D. Yield Sensitivity Analysis

We performed the yield sensitivity analysis at the centered solution obtained using six optimization variables.

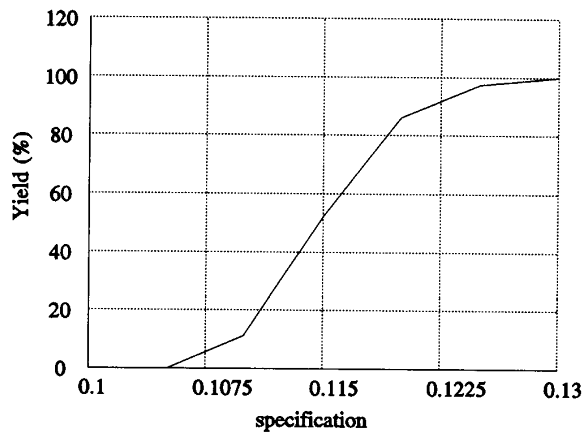

Fig. 6. Yield of the three-section microstrip transformer as a function of the specification imposed on $|S_{11}|$. High sensitivity of yield w.r.t. the specification can be observed. Yield is estimated with 250 Monte Carlo outcomes.

Fig. 6 shows yield as a function of the specification. The specification is swept from 0.10 to 0.13 with a 0.005 step. 250 Monte Carlo outcomes were used. The diagram confirms high sensitivity of yield w.r.t. the specification. The yield varies from 0 to 100 percent over a very small range of the specification.

We performed sensitivity analysis w.r.t. all six optimization variables using 250 statistical outcomes. As expected, the yield is very sensitive to the widths of all the sections and it is insensitive to the lengths of the sections. We also observed that the yield exhibits the highest sensitivity w.r.t. the width of the third section W_3. The analysis required very little additional computational effort. See Fig. 7 for the results.

V. YIELD OPTIMIZATION OF A SMALL-SIGNAL AMPLIFIER

The specification for a typical single-stage 6-18 GHz small-signal amplifier shown in Fig. 8 is

$$7 \text{ dB} \leq |S_{21}| \leq 8 \text{ dB from 6 to 18 GHz.}$$

The error functions for yield optimization are calculated at frequencies from 6 to 18 GHz with a 1 GHz step. The gate and drain circuit microstrip T-structures and the feedback microstrip line are built on a 10 mil thick substrate with relative dielectric constant 9.9.

First, we performed nominal minimax optimization using analytical/empirical microstrip component models. W_{g1}, L_{g1}, W_{g2}, L_{g2} of the gate circuit T-structure and W_{d1}, L_{d1}, W_{d2}, L_{d2} of the drain circuit T-structure were selected as optimization variables. W_{g3}, L_{g3}, W_{d3}, and L_{d3} of the T-structures, W and L of the feedback microstrip line, as

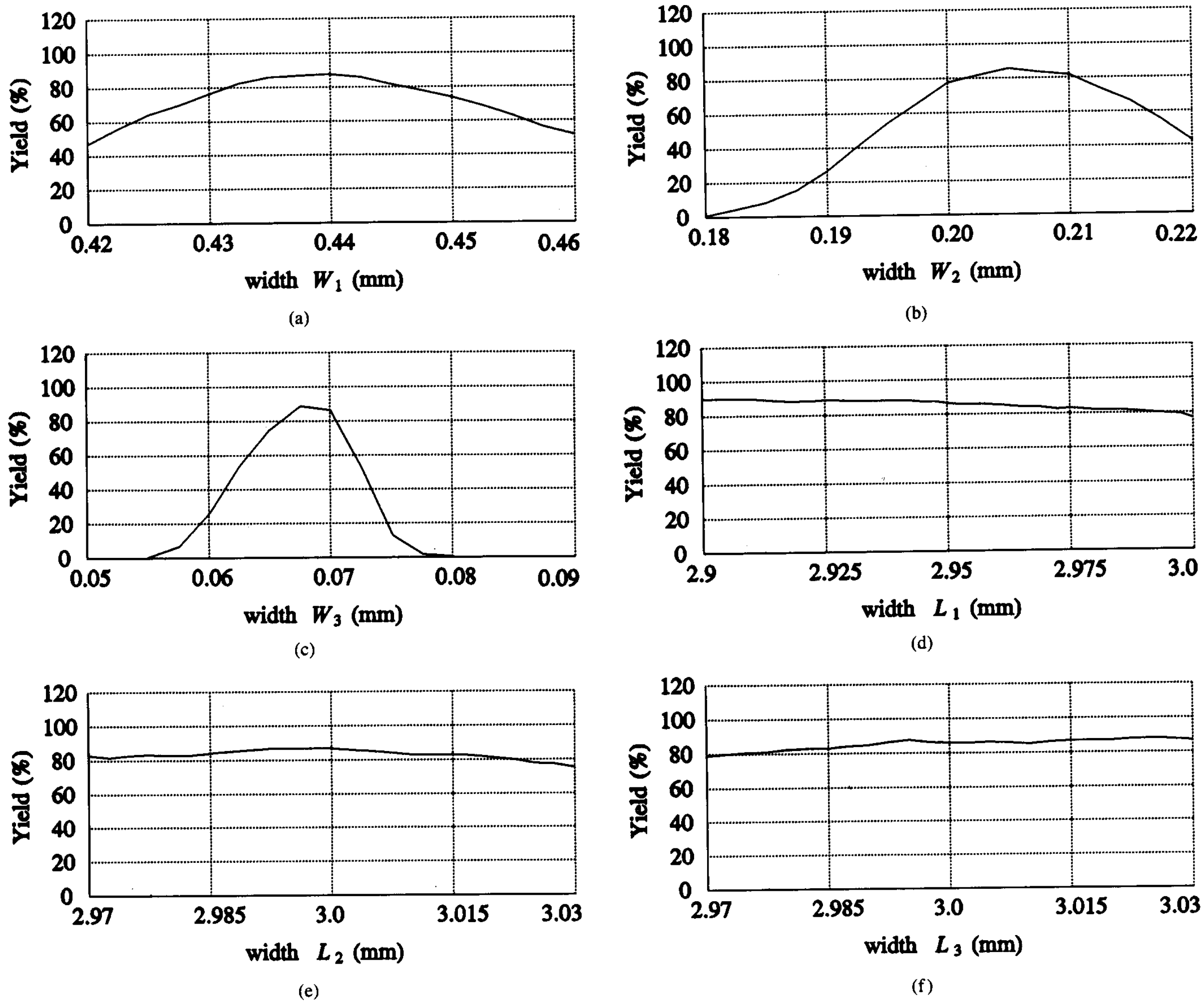

Fig. 7. Yield sensitivity analysis for the three-stage microstrip transformer at the centered solution. 250 Monte Carlo outcomes were used for yield estimation. The results are obtained with little additional computational effort. Yield as a function of (a) W_1, (b) W_2, (c) W_3, (d) L_1, (e) L_2, and (f) L_3.

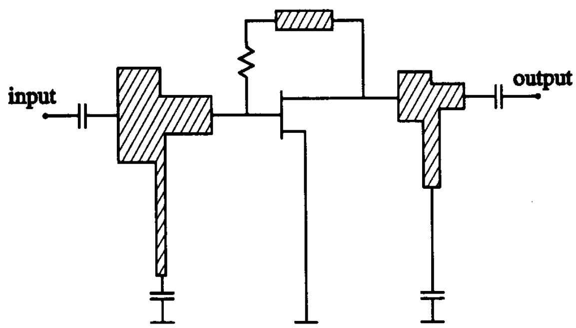

Fig. 8. Circuit diagram of the 6–18 GHz small-signal amplifier. We use ***em*** [7] to model the two *T*-structures and the microstrip line.

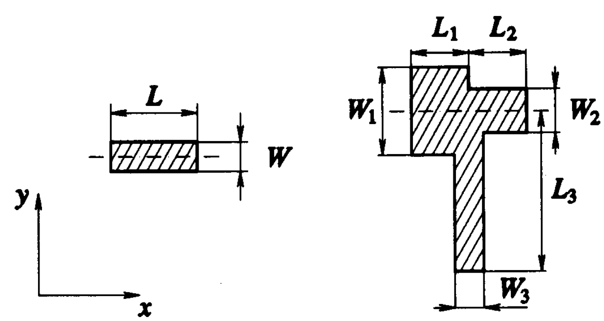

Fig. 9. Parameters of the feedback microstrip line and the microstrip *T*-structures.

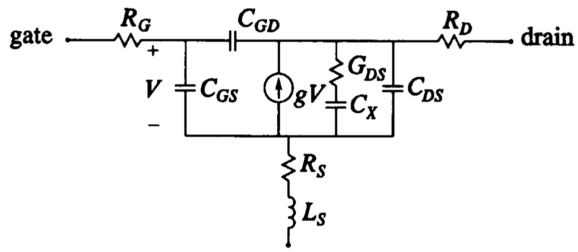

Fig. 10. Schematic diagram of the small-signal FET model. The value of the capacitor C_x is 2.0 pF. The transadmittance g is evaluated as $g = g_m e^{-2j\pi f\tau}$, where g_m and τ are given in Table III and f is the frequency.

TABLE III
EXTRACTED STATISTICAL DISTRIBUTIONS FOR THE FET PARAMETERS (FIG. 10)

FET parameter	Mean value	Standard deviation (percent)
R_G (Ω)	2.035	3
R_D (Ω)	3.421	8
R_S (Ω)	3.754	6
L_S (nH)	0.0811	7
G_{DS}(1/Ω)	0.00598	1
C_{DS}(pF)	0.06978	1
g_m	−0.0713	2
τ(ps)	1.9093	2
C_{GD}(pF)	0.02606	2
C_{GS}(pF)	0.30319	1.5

TABLE IV
EXTRACTED FET MODEL PARAMETER CORRELATIONS

	R_G	R_D	R_S	L_S	G_{DS}	C_{DS}	g_m	τ	C_{GD}	C_{GS}
R_G	1	−0.3121	−0.5869	0.5244	0.1914	−0.1805	−0.4473	−0.0567	−0.0971	−0.2548
R_D	−0.3121	1	0.7279	−0.7479	0.07056	0.411	0.3914	−0.047	−0.206	0.2474
R_S	−0.5869	0.7279	1	−0.8461	−0.0663	0.4825	0.6637	−0.2376	−0.1262	0.1974
L_S	0.5244	−0.7479	−0.8461	1	0.0162	−0.7326	−0.5204	0.02553	0.3676	−0.3084
G_{DS}	0.1914	0.07056	−0.0663	0.0162	1	0.1504	−0.5752	−0.2991	−0.171	0.3561
C_{DS}	−0.1805	0.411	0.4825	−0.7326	0.1504	1	0.1765	0.0295	−0.6786	0.1946
g_m	−0.4473	0.3914	0.6637	−0.5204	−0.5752	0.1765	1	−0.1781	0.0863	−0.3412
τ	−0.0567	−0.047	−0.2376	0.02553	−0.2991	0.0295	−0.1781	1	−0.2122	0.2624
C_{GD}	−0.0971	−0.206	−0.1262	0.3676	−0.171	−0.6786	0.0863	−0.2122	1	−0.2904
C_{GS}	−0.2548	0.2474	0.1974	−0.3084	0.3561	0.1946	−0.3412	0.2624	−0.2904	1

well as the FET parameters were not optimized. Fig. 9 shows the parameters of the T-structures and the microstrip line. Fig. 10 shows the small-signal FET model.

We assumed a 0.5 mil tolerance and uniform distribution for all geometrical parameters of the microstrip components. The statistics of the small-signal FET model were extracted from measurement data [11] and are given in Table III. The correlations among the FET model parameters are listed in Table IV. The value of the feedback resistor was 1600 Ω.

Monte Carlo simulation with 250 outcomes performed at the nominal solution with analytical/empirical microstrip component models reported 91 percent yield. To obtain a more accurate estimate, we used component level Q-models built from ***em*** [7] simulations for the microstrip components. The yield dropped to 55 percent. Fig. 11(a) and (b) show the Monte Carlo sweeps obtained using analytical/empirical and our ***em*** [7] based Q-models, respectively. Close similarities can be observed for lower frequencies, while discrepancies become larger for higher frequencies.

Utilizing the component-level quadratic Q-models built from ***em*** simulations, we further performed yield optimization of this amplifier. Yield estimated by 250 Monte Carlo simulations was increased to 82 percent. The corresponding Monte Carlo sweep diagram is shown in Fig. 12. Yield and the values of the optimization variables before and after optimization are given in Table V.

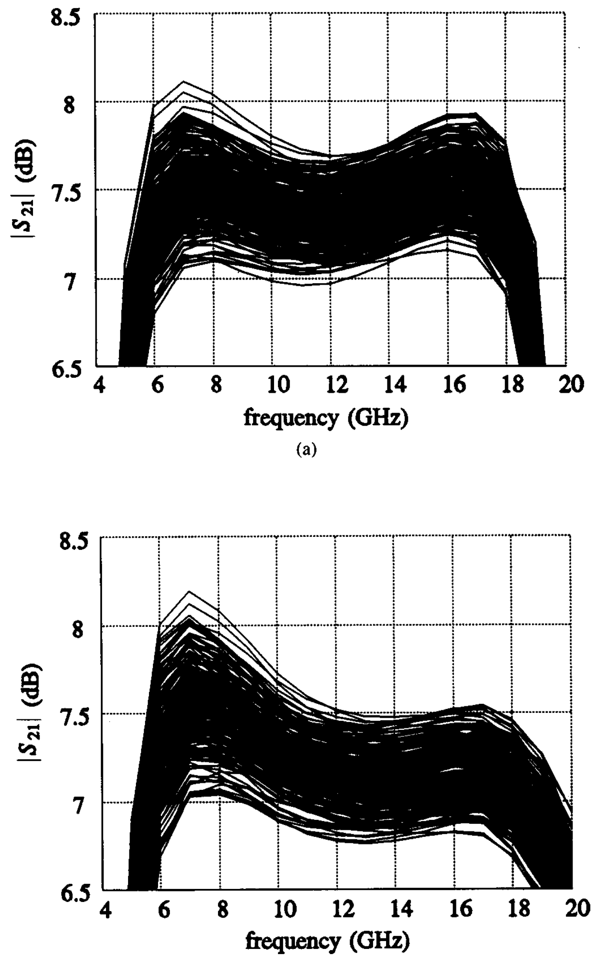

(a)

(b)

Fig. 11. $|S_{21}|$ of the small-signal amplifier for 250 statistical outcomes at the nominal minimax solution: (a) using analytical/empirical microstrip component models and (b) using ***em*** [7] based Q-models.

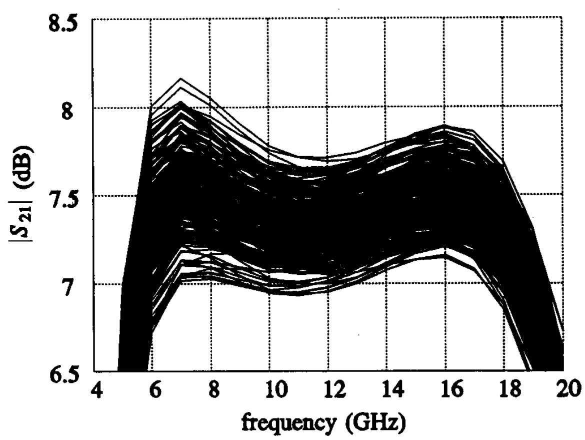

Fig. 12. $|S_{21}|$ of the small-signal amplifier for 250 statistical outcomes after yield optimization using ***em*** [7] based Q-models. Yield is increased from 55 to 82 percent.

TABLE V
MICROSTRIP PARAMETERS FOR THE AMPLIFIER

Parameters[a]	Nominal design	Centered design
W_{g1}	17.45	19
L_{g1}	35.54	34.53
W_{g2}	9.01	8.611
L_{g2}	30.97	32
W_{g3}	3[b]	3[b]
L_{g3}	107[b]	107[b]
W_{d1}	8.562	7
L_{d1}	4.668	6
W_{d2}	3.926	3.628
L_{d2}	9.902	11
W_{d3}	3.5[b]	3.5[b]
L_{d3}	50[b]	50[b]
W	2[b]	2[b]
L	10[b]	10[b]
Yield[c]	55 percent	82 percent

[a]Parameters are in mils. 0.5 mil tolerance and uniform distribution were assumed for all the parameters.
[b]Not optimized.
[c]50 outcomes were used in yield optimization and 250 outcomes for yield verification.

VI. CONCLUSIONS

We have presented a new multilevel quadratic modeling technique suitable for effective and efficient yield-driven design optimization. The method dynamically integrates the Q-models with database generation and updating, increasing both speed of processing and accuracy of the results. The approach is particularly useful for circuits containing complex subcircuits or components whose simulation requires significant computational effort. The efficiency of this technique allowed us to perform yield-driven design and analyze yield sensitivity for circuits containing microstrip structures accurately simulated by ***em*** [7]. We used a three-stage microstrip transformer and a small-signal amplifier to demonstrate the efficiency and accuracy of the method. Our approach significantly extends the microwave CAD applicability of yield optimization techniques.

ACKNOWLEDGMENT

The authors wish to thank Dr. J. C. Rautio of Sonnet Software, Inc., Liverpool, NY, for his initiatives and making ***em*** available for this work.

REFERENCES

[1] J. W. Bandler and S. H. Chen, "Circuit optimization: The state of the art," *IEEE Trans. Microwave Theory Tech.*, vol. 36, pp. 424–443, 1988.
[2] R. M. Biernacki and M. A. Styblinski, "Efficient performance function interpolation scheme and its application to statistical circuit design," *Int. J. Circuit Theory Appl.*, vol. 19, pp. 403–422, 1991.
[3] R. M. Biernacki, J. W. Bandler, J. Song, and Q. J. Zhang, "Efficient quadratic approximation for statistical design," *IEEE Trans. Circuits Syst.*, vol. 36, pp. 1449–1454, 1989.
[4] J. W. Bandler, R. M. Biernacki, S. H. Chen, J. Song, S. Ye, and Q. J. Zhang, "Gradient quadratic approximation scheme for yield-driven design," *IEEE MTT-S Int. Microwave Symp. Dig.*, Boston, MA, 1991, pp. 1197–1200.
[5] T. Itoh, Ed., *Numerical Techniques for Microwave and Millimeter-Wave Passive Structures*. New York: Wiley, 1989.
[6] R. H. Jansen and P. Pogatzki, "A hierarchically structured, compre-

hensive CAD system for field theory-based linear and nonlinear MIC/MMIC design," in *1992 2nd Int. Workshop German IEEE MTT/AP Joint Chapter Integrated Nonlinear Microwave and Millimeterwave Circuits Dig.*, Duisburg, Germany, 1992, pp. 333-341.

[7] *Em User's Manual* and *Xgeom User's Manual*. Sonnet Software, Inc., 135 Old Cove Road, Suite 203, Liverpool, NY, May 1992.

[8] *OSA90/hope*™, Optimization Systems Associates Inc., P.O. Box 8083, Dundas, Ont., Canada L9H 5E7, 1993.

[9] *Empipe*™, Optimization Systems Associates Inc., P.O. Box 8083, Dundas, Ont., Canada L9H 5E7, 1993.

[10] J. W. Bandler, S. H. Chen, and K. Madsen, "An algorithm for one-sided ℓ_1 optimization with application to circuit design centering," in *Proc. IEEE Int. Symp. Circuits Syst.*, Espoo, Finland, 1988, pp. 1795-1798.

[11] Measurement data provided by Plessey Research Caswell Ltd., Caswell, Towcester, Northamptonshire, England, 1990.

John W. Bandler (S'66-M'66-SM'74-F'78) was born in Jerusalem, on November 9, 1941. He studied at Imperial College of Science and Technology, London, England, from 1960 to 1966. He received the B.Sc. (Eng.), Ph.D. and D.Sc. (Eng.) degrees from the University of London, London, England, in 1963, 1967, and 1976, respectively.

He joined Mullard Research Laboratories, Redhill, Surrey, England in 1966. From 1967 to 1969 he was a Postdoctorate Fellow and Sessional Lecturer at the University of Manitoba, Winnipeg, Canada. He joined McMaster University, Hamilton, Canada, in 1969, where he is currently Professor of Electrical and Computer Engineering. He has served as Chairman of the Department of Electrical Engineering and Dean of the Faculty of Engineering. He currently directs research in the Simulation Optimization Systems Research Laboratory. He is President of Optimization Systems Associates Inc. (OSA), which he founded in 1983. OSA introduced the CAE systems RoMPE™ in 1988, HarPE™ in 1989, OSA90™ and OSA90/hope™ in 1991 and Empipe™ in 1992. He is also President of Bandler Research Inc., which he founded in 1989.

Dr. Bandler is a Fellow of the Royal Society of Canada, a Fellow of the Institution of Electrical Engineers (Great Britain), a member of the Association of Professional Engineers of the Province of Ontario (Canada), and a Member of the Electromagnetics Academy. He contributed to *Modern Filter Theory and Design*, Wiley-Interscience, 1973 and to *Analog Methods for Computer-Aided Analysis and Diagnosis*, Marcel Dekker, Inc., 1988. He has published more than 250 papers, four of which appear in *Computer-Aided Filter Design*, IEEE Press, 1973, one in each of *Microwave Integrated Circuits*, Artech House, 1975, *Low-Noise Microwave Transistors and Amplifiers*, IEEE Press, 1981, *Microwave Integrated Circuits*, 2nd ed., Artech House, 1985, *Statistical Design of Integrated Circuits*, IEEE Press, 1987, and *Analog Fault Diagnosis*, IEEE Press, 1987. He was an Associate Editor of the IEEE TRANSACTIONS ON MICROWAVE THEORY AND TECHNIQUES (1969-1974), Guest Editor of the IEEE TRANSACTIONS ON MICROWAVE THEORY AND TECHNIQUES Special Issue on Computer-Oriented Microwave Practices (March 1974) and Co-Guest Editor with R. H. Jansen of the IEEE TRANSACTIONS ON MICROWAVE THEORY AND TECHNIQUES Special Issue on Process-Oriented Microwave CAD and Modeling (July 1992). He joined the Editorial Boards of the *International Journal of Numerical Modelling* in 1987, and the *International Journal of Microwave and Millimeterwave Computer-Aided Engineering* in 1989.

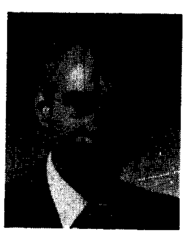

Radoslaw M. Biernacki (M'85-SM'86) was born in Warsaw, Poland. He received the Ph.D. degree from the Technical University of Warsaw, Warsaw, Poland, in 1976.

He became a Research and Teaching Assistant in 1969 and an Assistant Professor in 1976 at the Institute of Electronics Fundamentals, Technical University of Warsaw. From 1978 to 1980 he was on leave with the Research Group on Simulation, Optimization and Control and with the Department of Electrical and Computer Engineering, McMaster University, Hamilton, Ont., Canada, as a Postdoctorate Fellow. From 1984 to 1986 he was a Visiting Associate Professor at Texas A&M University, College Station. He joined Optimization Systems Associates Inc., Dundas, Ont., Canada, in 1986 as Senior Research Engineer. At OSA he has been involved in the development of commercial CAE software systems HarPE™, OSA90™, and OSA90/hope™ and related research on parameter extraction, statistical device modeling, simulation, and optimization, including yield-driven design of linear and nonlinear microwave circuits. In 1988 he also became a Professor (part-time) with the Department of Electrical and Computer Engineering, McMaster University. His research interests include system theory, optimization and numerical methods, and computer-aided design of integrated circuits and control systems.

Dr. Biernacki has authored or coauthored more than 80 publications and has been the recipient of several prizes for his research and teaching activities.

Shao Hua Chen (S'84-M'88) was born in Swatow, Guangdong, China, on September 27, 1957. He received the B.S. (Eng.) degree from the South China Institute of Technology, Guangzhou, China, in 1982, and the Ph.D. degree in electrical engineering from McMaster University, Hamilton, Ont., Canada, in 1987.

From July 1982 to August 1983, he was a teaching assistant with the Department of Automation, South China Institute of Technology. He was a graduate student with the Department of Electrical and Computer Engineering, McMaster University, from 1983 to 1987, during which time he was awarded an Ontario Graduate Scholarship for two academic years. He joined Optimization Systems Associates Inc., Dundas, Ont., Canada, in 1987 and engaged in commercial CAD software development. He has made major contributions to the development of the CAE systems HarPE™ and OSA90/hope™. Currently he is working as a Research Engineer in the Simulation Optimization Systems Laboratory, McMaster University. His professional research interests include optimization theory and implementation, CAD software architecture, device modeling, statistical simulation, circuit design centering, sensitivity analysis, computer graphics, and user interfaces.

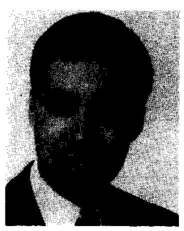

Piotr A. Grobelny was born in Zielona Gora, Poland, on September 18, 1962. He received the M.S. (Eng.) degree from the Technical University of Wroclaw, Wroclaw, Poland, in 1987.

From 1987 to 1990 he worked as a Research Assistant in the Machine Building Institute, Technical University of Wroclaw, where he was involved in the development of CAD and CAE software systems. In September 1990 he joined the Simulation Optimization Systems Research Laboratory and the Department of Electrical and Computer Engineering, McMaster University, Hamilton, Canada, where he is currently a teaching assistant and graduate student working towards the Ph.D. degree. He held an Ontario Differential Fee Waiver Award for the academic year 1990-1991. He has been awarded an Ontario Graduate Scholarship for the academic year 1993-1994. His research interests are in circuit CAD software design, simulation and optimization techniques, response function modeling techniques, sensitivity analysis, and yield optimization.

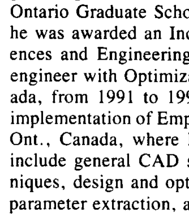

Shen Ye (S'88-M'92) was born in Shanghai, China, in 1957. He received the B.Eng. and M.Eng. degrees from Shanghai University of Technology, Shanghai, China, in 1982 and 1984, respectively, and the Ph.D. degree from McMaster University, Hamilton, Ont., Canada, in 1991, all in electrical engineering.

From 1984 to 1986, he was a teaching and research assistant with the Department of Electrical Engineering, Shanghai University of Technology. He joined the Simulation Optimization Systems Research Laboratory and the Department of Electrical and Computer Engineering, McMaster University as a graduate student in 1986. He held an Ontario Graduate Scholarship for the academic year 1989-1990. In 1991 he was awarded an Industrial Research Fellowship from the Natural Sciences and Engineering Research Council of Canada and was a research engineer with Optimization Systems Associates Inc., Dundas, Ont., Canada, from 1991 to 1993. He contributed substantially in the design and implementation of Empipe™. In 1993 he joined Com Dev Ltd., Cambridge, Ont., Canada, where he is a design engineer. His professional interests include general CAD software design, simulation and optimization techniques, design and optimization of microwave circuits, device modeling, parameter extraction, and statistical circuit design.